A sustainable solution for refrigeration using Thermo-acoustic technology
(March 2016)

L.K. Tartibu

Abstract—This work explores the use of thermo-acoustic coolers as alternative technology for refrigeration. A valid experimental evidence on the influence of the geometry of the honeycomb ceramic stack on the performance of thermos-acoustic refrigerators is described. Sixteen cordierite honeycomb ceramic stacks with square cross sections having four different lengths of 26 mm, 48 mm, 70 mm and 100 mm are considered. Measurements are taken at six different locations of the stack hot ends from the pressure antinode, namely 100 mm, 200 mm, 300 mm, 400 mm, 500 mm and 600 mm respectively. Measurement of temperature difference across the stack ends at steady state for different stack geometries are used to measure the performance of the device. The results with atmospheric air demonstrates the influence of the stack geometry on the cooling power and shows that some its geometrical parameters are interdependent.

***Index Terms*— Thermo-acoustic refrigerator, Stack, honeycomb ceramic, sound wave.**

1 INTRODUCTION

Thermo-acoustic refrigerators offer a solution to the current search for alternative refrigerants and alternative technologies (such as absorption refrigeration, thermoelectric refrigeration and pulse-tube refrigeration) necessary to reduce harsh environmental impact [1]. Thermo-acoustics is a field of study that combines both acoustic waves and thermodynamics. The interaction of the temperature oscillation accompanied by the pressure oscillation in a sound wave with solid boundaries initiates an energy conversion processes. In ordinary experience, this interaction between heat and sound cannot be observed. But it can be amplified under suitable conditions to give rise to significant thermodynamic effects such as convective heat fluxes, steep thermal gradients and strong sound fields. Thermo-acoustic refrigerators (TARs) use acoustic power to cause heat flow from a low temperature source to high temperature sink [2].

Thermo-acoustic refrigerators (Fig. 1) consist mainly of a loudspeaker (a vibrating diaphragm or Thermo-acoustic prime mover) attached to a resonator filled with gas, a stack usually made of thin parallel plates, and two heat exchangers placed at either side of the stack. The stack forms the heart of the refrigerator where the heat-pumping process takes place, and it is thus a critical element for determining the performance of the refrigerator [3]. For the temperature gradient along the stack walls to remain steady, the material selected should have higher heat capacity and lower thermal conductivity than the gas; otherwise the stack won't be affected by the temperature oscillations of the nearby gas. In addition, a material of low thermal conductivity should be chosen for the stack and the resonator to prevent leaking from the hot side of the resonator back to the cold side and to withstand higher pressure [4].

L.K. Tartibu, Mechanical Engineering Technology Department, University of Johannesburg, Doornfontein Campus, Johannesburg 2028, South Africa (e-mail: ltartibu@uj.ac.za).

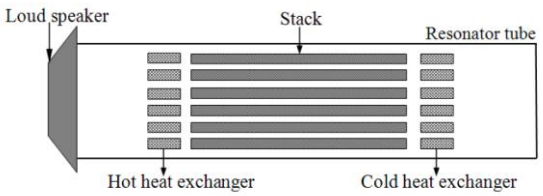

Fig. 1: Schematic diagram of a typical Thermo-acoustic refrigerator

Using a sound source such as a loudspeaker, an acoustic wave is generated to make the gas resonant. As the gas oscillates back and forth within the chamber, the standing sound wave creates a temperature difference along the length of the stack. This temperature change is a result of compression and expansion of gas by sound pressure and thermal interaction between the oscillating gas and the surface of the plate. Heat is exchanged with the surroundings through heat exchangers at the cold and hot side of the stack [2]. The basic mechanics behind Thermo-acoustics are already well-understood. A detailed explanation of the way Thermo-acoustic coolers work is given in Refs [3] and [5]. Recent research focuses on improving the performance of the devices so that Thermo-acoustic coolers can compete with commercial refrigerators. One way to improve the performance of current devices is by understanding interactions between design parameters experimentally.

Due to the critical nature of the interaction between the gas and solid material forming the stack, there have been a number of studies focused on the selection and optimisation of the stacks for standing-wave refrigerators. Typically, stacks with regular geometrical configurations, for example parallel-plate type [2], offer excellent performance. However, such stacks are too costly and too difficult to make, especially when the channel size goes down into tens of microns range. Similarly, there seem to be very few commonly available materials for such stacks. Therefore, a common practice in Thermo-acoustics is to use ceramic substrate with square pores. The idea behind

the current research is to investigate the influence of such accessible materials for a potential use as stacks.

2 MOTIVATIONS

To evaluate the thermal performance, the temperature difference across the stack end temperature is the main focus of the present work. Several authors [6], [7], [8], [9] have studied the influence of the temperature difference at the stack extremities either mathematically, numerically or experimentally in an effort to improve the performance of Thermo-acoustic refrigerators through the use of optimisation. An important findings reported by Hariharan and Sivashanmugam [10] and Tartibu et al. [11] [12] show that geometrical design parameters are interdependent.

Therefore, the present work use different honeycomb ceramic stacks geometry and aims to investigate the temperature difference across the stack ends with the objective of highlighting the influence and the interdependency of the stack parameters (length, pore size and position) on the performance of the device. Section 3 describes the experimental set-up and apparatus used. Detailed description of the geometry of stacks used in the experiment is provided. Section 4 present and discuss the results obtained for each study. Temperature differences obtained are reported. Section 5 reports the contributions of this work.

3 EXPERIMENTAL INVESTIGATION

3.1. Experimental set-up

The main objectives of this experimental scheme are to obtain the following characteristics of the stack:

- Measurements of temperature difference (ΔT) obtained across the stack ends at steady state for different stack geometries (lengths of the stacks varying from 26 to 100 mm) and stack spacing (homogenous stacks ranging from 64 to 300 Cells Per Square Inch, or CPSI).
- Measurements of the temperature difference (ΔT) obtained across the stack ends at steady state for different positions of the stack (the hot end of the stack varies from 100 to 600 mm from the closed end).

The TAR experimentation was carried out using a quarter-wavelength resonator design. A speaker-driven system was used to ensure equal acoustic environments for each test instead of a heat driven one.

An experimental set-up (Thermo-acoustic refrigerator) (Fig. 2) for measuring the performance of the device function of the geometry of the stack has been designed and assembled. The set-up has the following components:

- a resonator tube;
- a loudspeaker; and
- a stack.

As this set-up does not have hot heat exchanger and cold heat exchanger at the ends of the stack, it is similar to a Thermo-acoustic couple (TAC). For this study, the stack is not cooled actively. The main function of this experiment is to investigate the stack geometry, rather than achieving highest temperature drop or cooling power.

The resonator is an acrylic tube (thermal conductivity 0.20 W/m K at 23oC) of a length of 780 mm and an inner diameter of 44 mm. The resonator is filled with air at atmospheric pressure. The position of the stack can be adjusted at any location on the resonator. One end of the tube is closed with an end cap. At the other end, a commercially available loudspeaker (4 Ω) constitutes the acoustic power source (driver). The loudspeaker has a frequency range of 45 – 26000 Hz and 180 W maximum acoustic power output.

This driver is located in PVC housing (130×130×72 mm) to which the resonator is connected. A function generator (model Agilent 33220A) and an 80 W amplifier have been used to drive the system at the operating frequency and with the selected power

The accuracy of the amplitude and the frequency of the output signal are 0.1mV and 1μHz, respectively.

The stacks studied in the measurement set-up are prefabricated stacks made of 64, 100, 230 and 300 CPSI respectively, manufactured by Applied Ceramics Inc. [13]. The cordierite honeycomb ceramic is selected because of its low thermal conductivity, high surface area for conversion efficiency, high thermal capability (up to 1400^0C), ability to sustain large temperature gradients and highest sound pressure level output. Additionally, such stacks are relatively cheaper and easier to make, especially when the channel size goes down into tens of microns range.

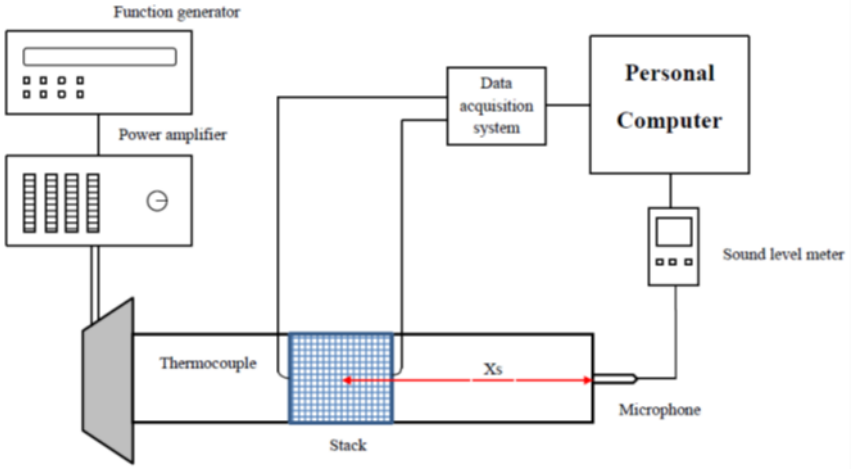

Fig. 2. A schematic diagram of experimental apparatus.

Sixteen cordierite honeycomb ceramic stacks with square cross sections (as shown in Fig. 3) having four different lengths - 26 mm, 48 mm, 70 mm and 100 mm – , cut with a hacksaw blade and polished with a sand paper, are considered. Cordierite honeycomb ceramic stack properties and specifications are provided in Table I. Cordierite ceramic is type of Alumina magnesia Silicate. It offers excellent thermal shock resistance and high temperature resistance up to 1200°C. Honeycomb Cordierite ceramic parts have been widely used in catalytic converter, catalyst support, high temperature gas filtration, flame diffusion to reduce volatile organic compounds, nitrogen oxide emission and remove particulates from flue gas stream. Measurements are taken at six different locations of the stack hot ends from the pressure antinode, namely 100 mm, 200 mm, 300 mm, 400 mm, 500 mm and 600 mm respectively.

3.2. Experimental apparatus

A variety of equipment is utilised to perform the measurements. Thermocouples are used to measure thermal response, and pressure measurements are made with a sound level meter, while a data acquisition system records the measurements (as shown in Fig. 2).

A common method to record temperature is through the use of thermocouples. K-Type thermocouples wires have been selected for this work. They are made of chromel and alumael from National Instruments [14]. Based on National Instruments, these exposed junction type thermocouples which feature fiberglass insulation (melting point 482ºC) allow for a temperature range of 0ºC to 482ºC. The accuracy of the thermocouple is ± 2.2ºC [14].

Table I: Properties and dimensions of stack materials [13]

Material: Cordierite Ceramic Honeycomb				
Density [Kg/m^3]	2500			
Thermal conductivity [W/m K]	0.42			
Specific heat [J/Kg K]	1047			
Melting point [ºC]	1450			
Coefficient of thermal expansion ºC×10^{-6}	0.7			
	Refrigerator			
Stack Lengths [mm]	100			
	70			
	48			
	26			
Stack position (from closed end) [mm]	100			
	200			
	300			
	400			
	500			
	600			
	Size (pore sizes)			
	Size 4: 64 CPSI	Size 3: 100 CPSI	Size 2: 230 CPSI	Size 1: 300 CPSI
Plate thickness [mm]	0.690	0.550	0.160	0.140
Plate spacing [mm]	3.175	2.540	1.675	1.467
Porosity [BR]	≈0.8	≈0.8	≈0.9	≈0.9

Fig.3: Stack samples used in the experiments/ TAR

The acoustic pressure measurements are made by a sound level meter (Lutron SL 4013) which, when placed near the driver end, measures the dynamic pressure (P_0). The drive ratio (DR) is evaluated using this dynamic pressure measurement. The accuracy of the sound level meter, as indicated by Lutron Electronic [15] is ±1.5 dB. To convert the sound level meter data from decibel (dB) to Pascal (Pa), the following expression is used:

$$L_P = 10\log_{10}\left(\frac{P^2}{P_{ref}^2}\right) = 20\log_{10}\left(\frac{P}{P_{ref}}\right)\text{dB} \quad (1)$$

where L_P =sound pressure level in dB

P =root mean square sound pressure = $\frac{P_0}{\sqrt{2}}$

P_{ref} =20×10^{-6} Pa or 20 µPa = reference pressure

The analog signals generated by sensors are obtained using data acquisition (DAQ) hardware (as shown in Fig. 2). Once these signals are interpreted by the DAQ, a digital signal is sent to a computer for processing, recording and analysing. Although there are numerous possible solutions for acquiring and processing analog data, LabVIEW 11 [16] has been selected as the environment for data visualisation and processing, together with a National Instruments (NI) DAQ hardware (NI USB-9211A).
A portable USB based DAQ is chosen for thermocouple measurement (National instruments hardware NI USB-9211). The sound level meter is a portable five digits, compact sized, digital display sound level meter designed for long term measurements, with an operating environment of 0 to 50°C.

4. RESULTS

4.1 Temperature behaviour as a function of driving frequency

In this set of experiments, the effect of the driving frequency on the temperature difference across the stack was investigated. During these experiments, the hot end of a 100 mm stack (size 2) remained 100 mm from the closed end and the function generator voltage was kept at 150 mV_{RMS}. The data for this test was collected beginning at 50 Hz and ranging up to 350 Hz in increments of 5 Hz. The response time of the temperature was much slower than the pressure amplitude; hence, each frequency was maintained for approximately 250 to 350 seconds. Fig. 4 illustrates the hot side temperature, the cold side temperature and the temperature difference across the stack end as obtained and recorded in this study. This slow response time of the temperature measurement may be due to the lack of good insulation. In this experiment, the resonator tube is not insulated and heat is transferred between inside and outside the resonator tube.

In connection with the acoustic amplitude, the pressure amplitudes within the thermo-acoustic resonator are only a small fraction (typically 5%) of the static internal pressures that are approximately 10 to 30 atmospheres. Given the relatively small acoustic pressure amplitudes, a pressure vessel that is strong enough to safely contain the static pressure cannot yield enough under the acoustic pressure variations to radiate much sound to the environment. The perceptible acoustic radiation was due to the small vibration of the resonator. The sound pressure level recorded at one meter away was less than 60 dB in these experiments.

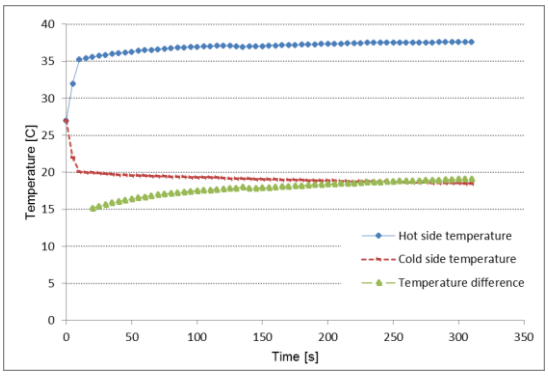

Fig. 4: Hot side and cold side temperature across the ceramic stack/TAR

A second test was run with a frequency increment of 1 Hz, starting at 130 Hz and ranging beyond the first peak (140 Hz) in order to illustrate a more exact picture of the temperature behaviour in the range of frequencies present in the first peak. Fig. 5 shows the temperature difference for the entire range of frequencies. The optimal driving frequency identified results in the highest temperature difference across the stack, as suggested by previous studies [9]. The total length of this TAR set-up was 780 mm, which corresponds to an optimal operating frequency of $c/\lambda \approx 110$ Hz (with c representing the sound speed and λ is the wavelength corresponding to 4 × resonator length). This is not in agreement with the results reported in Fig. 5 evaluating the standing wave resonator frequency at 135 Hz. Similar findings are reported by Ref [17]. It is suggested that the frequency of the peak temperature difference won't be in satisfactory agreement with the system resonance frequency if the stack position is not optimum. Therefore, all remaining results were taken under the same operating conditions, with the driving frequency fixed at 135 Hz.

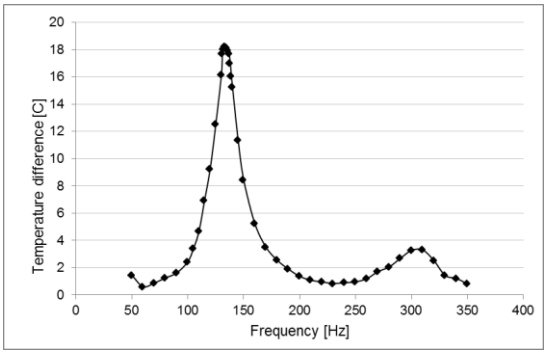

Fig.5: Temperature difference function of the frequency

4.2 Temperature behaviour as a function of power input

In this set of experiments, the effect of the output voltage of the function generator and the power input on the temperature difference across the stack was investigated. During these experiments, the hot end of a 100 mm stack (size 2) remained 100 mm from the closed

end and the frequency of the acoustic wave was kept at 135 Hz. The experiments were carried out at eight different function generator output voltages ranging from 50 mV_{RMS} to 500 mV_{RMS} corresponding to eight different power inputs, ranging from 5 W to 18 W. During each experiment, the temperature was measured at both ends of the stack, with results revealed in Fig.s 6 and 7. The plots show that the temperature difference across the stack is larger for the output voltage of 250 mV_{RMS}. Therefore, the generator output voltage has been set to 250 mV_{RMS} corresponding to 18.5 W for the remainder of the experiments.

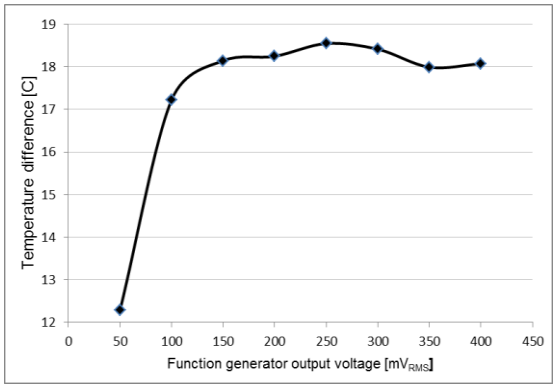

Fig.6: Temperature difference across the stack ends versus the function generator output voltage

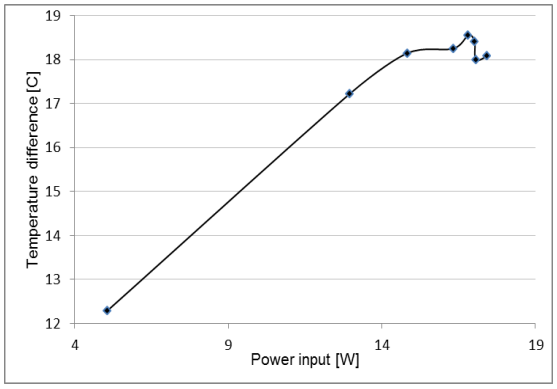

Fig.7: Temperature difference across the stack ends versus the power input

4.3 Temperature behaviour as a function of stack length

The influence of the stack length on the temperature difference was also studied. For this investigation, four different sizes of ceramic stacks (64 CPSI, 100 CPSI, 230 CPSI and 300 CPSI) having four different lengths (26 mm, 48 mm, 70 mm, and 100 mm) were used. Figs 8 through 11 show the temperature difference as a function of the stack length corresponding respectively to size 1, size 2, size 3 and size 4. It shows that there is a peak in temperature difference corresponding to the optimal stack length in each configuration. The highest temperature peaks obtained for size 1, size 2 and size 3 were 13.147°C, 19.136 °C and 14.722 °C respectively, corresponding to a 70 mm stack. However, a maximum temperature of 10.552 °C has been obtained with a 48 mm stack of size 4. These results demonstrate that there is no clear trend of temperature difference function of the stack length.

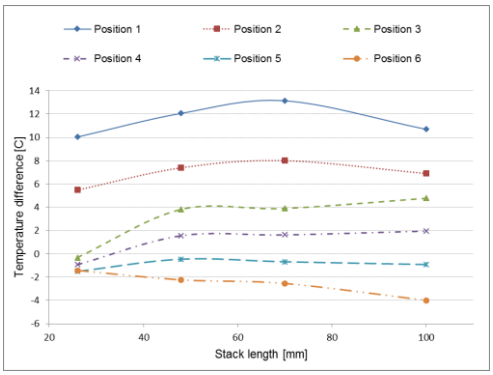

Fig. 8: Temperature behaviour as a function of stack length/size 1

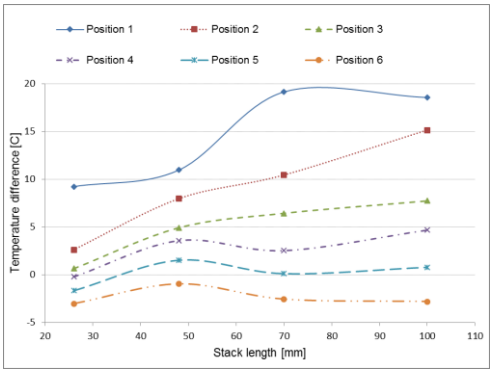

Fig. 9: Temperature behaviour as a function of stack length/size 2

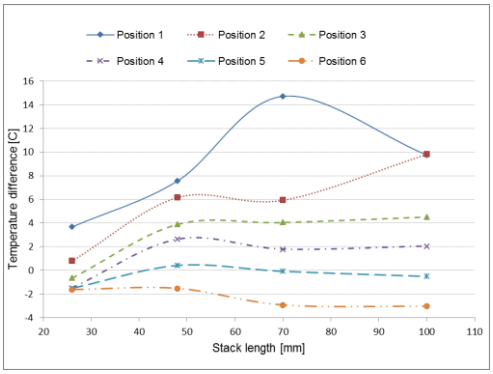

Fig. 10: Temperature behaviour as a function of stack length/size 3

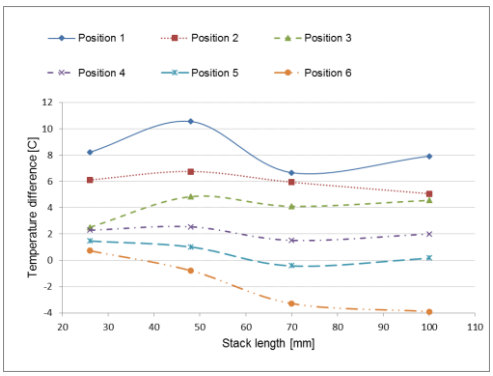

Fig. 11: Temperature behaviour as a function of stack length/size 4

4.4 Temperature behaviour as a function of stack position

The influence of stack locations on the temperature difference was studied. The stack location is measured relative to the closed end of the resonator. For good resolution, this study was conducted at six locations, starting at 100 mm to 600 mm from the closed end (Table 1). The temperature difference between the two ends was used as the indicator for optimal placement. Figs. 12 through 15 show this temperature difference as a function of the stack location. A logarithmic curve fit is shown for visual guidance, allowing for a peak in temperature difference to suggest positioning the stack closer to the pressure antinode which is in complete agreement with previous studies [8]. Additionally, locating the stack further away from the closed end results in an obvious drop in temperature difference because of the decrease in pressure amplitude away from the pressure antinode.

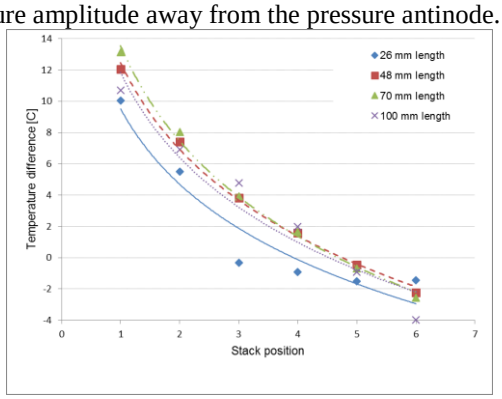

Fig. 12: Temperature behaviour as a function of stack position/size 1

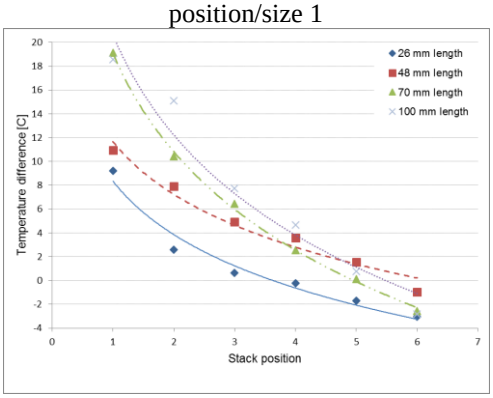

Fig.13: Temperature behaviour as a function of stack position/size 2

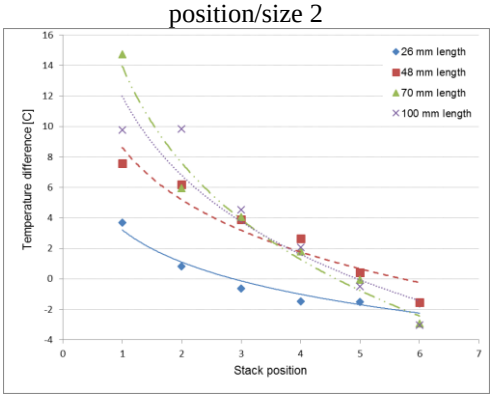

Fig. 14: Temperature behaviour as a function of stack position/size 3

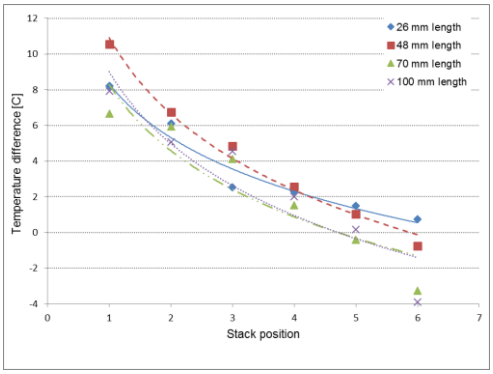

Fig.15: Temperature behaviour as a function of stack position/size 4

4.5 Temperature behaviour as a function of stack pore size

The influence of the stack spacing was studied. The gas thermal penetration depth (δ_k) has been evaluated to 0.214 mm. Although Tijani et al. [4] recommend a spacing of 2 to 4 δ_k for optimal transfer between the gas and the surface of the stack, this experimental investigation was performed with stacks having larger spacing (Table 1) as per the experimental objectives. The results found in Fig. 16 and 17 suggest a peak of temperature difference for size 1 corresponding to 10.044 ^{o}C and 12.067 ^{o}C respectively. These results show a similar trend for the 26 mm and the 48 mm stacks. However, different profiles are observed from the results reported in Figs 18 and 19. The highest temperature difference is observed for size 2. The temperature differences of 19.136 ^{o}C and 18.547 ^{o}C corresponding respectively to 70 mm and 100 mm stacks have been measured.

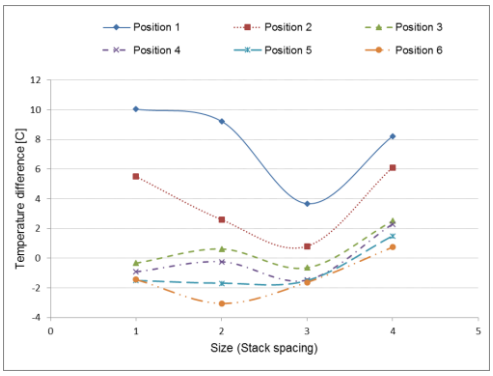

Fig.16: Temperature behaviour as a function of pore size/26 mm

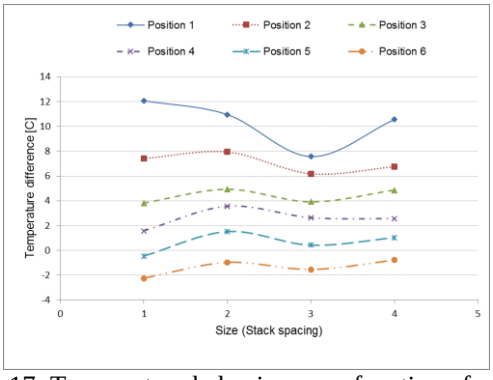

Fig.17: Temperature behaviour as a function of pore size/48 mm

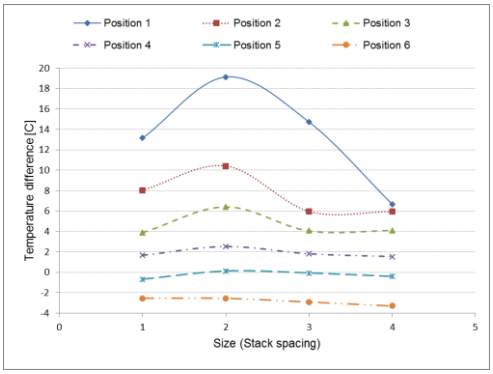

Fig.18: Temperature behaviour as a function of pore size/70 mm

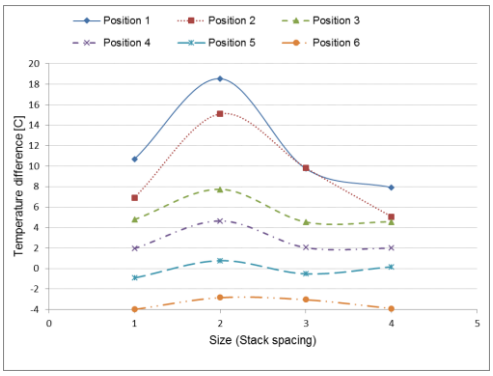

Fig.19: Temperature behaviour as a function of pore size/100 mm

Figs 8 to 19 demonstrate that the magnitude of maximum temperature difference generated at the stack ends depends on the geometry and the position of the stack.

5. CONCLUSION

This work demonstrates experimentally the potential of Thermo-acoustic refrigerator as possible alternative for refrigeration. In order to investigate the influence of stack geometry and position on the performance of the device, an acoustically-driven Thermo-acoustic refrigerator was built. This system utilises a loudspeaker to create strong sound waves in a quarter wavelength resonator. Sixteen different cordierite honeycomb ceramic stacks of four different pore sizes were investigated. These stacks were moved successively at six different locations inside the resonator. The temperature differences across the stack in each configuration were used to measure the performance of the refrigerator. The influence of the stack length, the stack position and the stack pore sizes reveal that there is a peak of temperature difference. The results suggest that the stack should be located closer to the pressure antinode for maximum temperature difference in all cases. However, the stack length and the stack pore sizes cannot be treated independently based on the profile of the temperature differences measured. This study reveals that these parameters are indeed interdependent.

ACKNOWLEDGEMENTS

This research was supported by the Research office of Mangosuthu University of Technology, the department of Mechanical Engineering of Cape Peninsula University of Technology and the Faculty of Engineering of the University of Johannesburg, Johannesburg, South Africa.

6. REFERENCES

[1] Y. K. Joshi and S. V. Garimella, “Thermal challenges in next generation electronic systems”. Microelectronics journal, vol. 34, no. 3, pp. 169. 2003.

[2] G. W. Swift, “Thermoacoustics: a unifying perspective for some engines and refrigerators”. Acoustical society of America, Melville NY. 2000.

[3] G. W. Swift, “Thermoacoustic engines”. Journal of acoustical society of America, vol. 4, pp. 1146–1180. 1988.

[4] M. E. H. Tijani, J. C. H. Zeegers and A. T. A. M. De Waele, “Design of thermoacoustic refrigerators”. Cryogenics, vol. 42, no. 1, pp. 49-57. 2002.

[5] J. C. Wheatley, T. Hofler, G. W. Swift, A. Migliori, “Understanding some simple phenomena in thermoacoustics with applications to acoustical heat engines”. American journal of physics, vol. 53, pp. 147–162. 1985.

[6] Q. Tu, Z. J. Chen and J. X. Liu. “Numerical simulation of loudspeaker-driven thermoacoustic refrigerator”. Proceedings of the twentieth International cryogenic engineering conference (ICEC 20). 2005. Beijing, China.

[7] M. Akhavanbazaz, M. H. Kamran SiddiquI and R. B. Bhat, “The impact of gas blockage on the performance of a thermoacoustic refrigerator”. Experimental thermal and fluid science, vo. 32, no. 1, pp. 231-239. 2007.

[8] M. Wetzel and C. Herman, “Design optimisation of thermoacoustic refrigerators”. International journal of refrigeration, 1997, vol. 20, no. 1, pp. 3-21. 1997.

[9] L. K. Tartibu, “A multi-objective optimisation approach for small-scale standing wave thermoacoustic coolers design”. Doctoral thesis. Cape Peninsula University of Technology. Cape Town, South Africa. 2014.

[10] N. M. Hariharan and P. Sivashanmugam, “Optimization of thermoacoustic refrigerator using response surface methodology”. Journal of hydrodynamics, vol. 25, no. 1, pp. 72-82. 2013.

[11] L. K. Tartibu, B. Sun and M. A. E. Kaunda, “Lexicographic multi-objective optimisation of thermoacoustic refrigerator’s stack”. Journal of heat and mass transfer, vol. 51, no. 5, pp. 649-660. 2015.

[12] L. K. Tartibu, B. Sun and M. A. E. Kaunda, “Optimal design study of thermoacoustic regenerator with lexicographic optimisation method”. Journal of engineering, design and technology, vol. 13 no. 3, pp. 499 – 519. 2015.

[13] Applied Ceramics Inc. (2011). Versagrid™ Product Offering, viewed 10 September 2013, from http://appliedceramics.com/products_versagrid.htm

[14] National Instruments. (n.d). Thermocouple and RTD sensors, viewed 10 September 2013, from http://www.ni.com/pdf/products/us/3daqsc350-351.pdf.

[15] Lutron Electronic. (n.d). Sound level meter model SL-4013, viewed 10 September 2013, from http://www.instrumentsgroup.co.za/index_files/Lutron/database/pdf/SL-4013.pdf.

[16] National Instruments. (2011). http://www.ni.com/labview/.

[17] Yong Tae Kim and Min Gon Kim, “Optimum positions of a stack in a thermoacoustic heat pump”. Journal of the Korean physical society, vol. 36, no. 5, pp. 279-286. 2000.

AUTHORS BIOS AND PHOTOGRAPHS

Lagouge Tartibu holds a Doctorate degree in Mechanical Engineering from Cape Peninsula University of Technology since 2014. He is a Senior Lecturer in the department of Mechanical Engineering Technology at the University of Johannesburg. His research interest includes Applied Thermal Engineering, Thermo-acoustic technology, mathematical analysis and optimization and vibration analysis. He is a member of the South African Institution of Mechanical Engineering (SAIMECHE) and the International Association of Engineers (IAENG).